ELSEVIER

Segregation of drop size and velocity in jet impinging splash-plate atomizers

N. Ashgriz, R. Washburn, and T. Barbat
Department of Mechanical and Aerospace Engineering, State University of New York at Buffalo, Buffalo, NY

Atomization of a liquid jet as it impinges on the flat end of a circular rod (splash plate) is studied experimentally. The effects of the splash-plate diameter (surface diameter) and the jet velocity on the disintegration of the jet are investigated. Six surface-to-jet diameter ratios of 2.3, 3.0, 5.1, 5.3, 8.7, and 13.9 are used, while the jet velocity is varied from 7.4 to 31 m/s. A hollow cone sheet and consequently a spray are formed as a result of this type of impingement. A phase Doppler particle analyzer (PDPA) is used to measure the diameter and velocity variations in the resulting sprays simultaneously. The diameter and velocity of the drops at the region of the spray with the highest volume flux are measured for various surface diameters and the jet velocities. It is found that the mean diameter of the drops at this region decreases as the jet velocity increases. In addition, at low jet velocities ($u_j <$ 18 m/s), the mean drop diameter increases with an increase in the surface to jet diameter ratio; however, at high jet velocities ($u_j > 18$ m/s), it is insensitive to the changes in the surface to jet diameter ratio. Empirical correlations are derived and reported for these variations. It is also found that the mean drop diameter and velocity are the largest at the outer edges of the spray, and they continuously decrease across the spray toward the spray axis. This result indicates that the impinging jet atomizers segregate drop sizes and velocities. The suspected cause of this segregation is the flow currents inside the hollow cone spray.

Keywords: atomization; splash plate; impinging jets; size distribution

Introduction

Impinging jet atomizers can be divided into two general categories: the jet-on-jet and jet-on-surface impinging or splash-plate atomizers. Jet-on-jet impinging atomizers are typically used in liquid propellant rocket engines where fast mixing between liquid fuel and liquid oxidizer is essential (Heidemann et al. 1957; Taylor 1960; Ibrahim and Przekwas 1991; Vassallo et al. 1992; Ryan et al. 1995). Jet-on-surface impinging atomizers are commonly used in devices where a large diameter orifice is needed to either provide a large mean flow rate, such as in fire sprinklers, or where a highly viscous fluid is used, such as in coal slurry fuel injectors. In such sprays, the liquid jet emerges from a large orifice and impinges on a solid surface (splash plate). Because of the wide-spread application, the impinging jet atomizers have been extensively investigated. Detailed studies of these atomizers were initiated by Hagerty and Shea (1955) and Dixon et al. (1952). Later Dombrowski and Hooper (1963), Huang (1970), and Donaldson and Snedecker (1971) contributed to the further understanding of this problem.

Hagerty and Shea (1955) and Fraser et al. (1962) described the instability and breakup of liquid sheets as follows. The fluid sheet experiences disturbances due to the aerodynamic forces. Consequently, the sheet becomes wavy, the amplitudes of the waves grow and cause the sheet to break up into ligaments. Finally, the liquid ligaments break up into drops based on the Rayleigh (1945) theory (see also Ashgriz and Mashayek 1995). By assuming an exponential growth rate for the amplitude of the wavy liquid sheet, Fraser et al. derived the following equation to predict the mean drop diameter in the spray.

$$d = \text{const}\left(\frac{\rho_l}{\rho_a}\right)^{1/6}\left(\frac{k_o\gamma}{\rho_l u_j^2}\right)^{1/3} \tag{1}$$

where d is the mean drop diameter in the spray, ρ_l and ρ_a are the liquid and ambient air densities, respectively, k_o is a constant for the nozzle, γ is the surface tension coefficient, and u_j is the jet velocity. Ingebo (1984) made drop size measurements of the spray from a jet impinging splash-plate atomizer by using photographic techniques. He derived the following empirical equation for the mean diameter of the drops in quiescent air:

$$d = \frac{d_j}{2.8\times 10^{-4}\,\text{Re}_j} \tag{2}$$

where d_j is the jet diameter and $\text{Re}_j = \rho_l u_j d_j/\mu_l$ is the liquid jet Reynolds number with μ_l being the liquid viscosity. Note that in Equation 1, which is for the breakup of a liquid sheet, the drop

Address reprint requests to Prof. N. Ashgriz, Mechanical and Aerospace Engineering, SUNY at Buffalo, Clifford C. Furnas Hall, Box 604400, Buffalo, NY 14260-4400, USA.

Received 7 October 1995; accepted 23 April 1996

Int. J. Heat and Fluid Flow 17: 509–516, 1996

655 Avenue of the Americas, New York, NY 10010

0142-727X/96/$15.00
PII S0142-727X(96)00059-7

diameter is proportional to $u_j^{-2/3}$; whereas, in Equation 2, which is for the splash-plate atomization, the drop diameter is proportional to u_j^{-1}. Therefore, it appears that for the same jet velocity the splash plate reduces the mean drop diameter.

This paper presents a detailed investigation of the impinging jet atomization. Spray characteristics—namely, mean drop diameter, mean velocity, and volume flux—are measured at different locations in the spray as opposed to measuring the mean values for the entire spray. The effects of the splash-plate diameter and the impinging jet velocity on the spray characteristics are investigated.

Experimental setup

The atomizer is designed so that both the liquid jet and the splash plate can be changed independently. The liquid jet injector consists of a 0.16-cm outer diameter hypodermic tube connected to a 0.64-cm diameter, 10.16-cm long stainless steel tube by a brass connector. The diameter of the liquid jet can be changed by using a hypodermic tube with a different inner diameter. The injector is mounted onto a platform that allows its vertical and horizontal position to be aligned so that the jet impinges on the center of the impingement surface. The impingement surface is the flat end of a circular rod. Different rod diameters of $d_s = 1.39$, 2.33, 4.01, and 6.30 mm are used. They are made of aluminum and copper and machined to produce a smooth surface and to remove impurities that can affect the results, from the surface, such as corrosion or oils. Two jet diameters of $d_j = 0.46$ mm and 0.93 mm are used. When the jet strikes the center of the impingement surface, an axisymmetric conical sheet and, consequently, an axisymmetric spray are produced. Six different combinations of surface to jet diameter ratios of $\Delta = d_s/d_j = 2.3$, 3.0, 5.1, 5.3, 8.7, and 13.9 are tested. The smaller jet is used to obtain jet velocities from 12 to 31 m/s, while the larger jet generates a range of jet velocities from 7.4 to 9.7 m/s. The jet Reynolds numbers range from 6000 to 14,000, and the appearance of the jet is wavy and turbulent, which indicates that the flow is in the transition or turbulent flow regime.

The fluid pumping system consists of a driving force, a holding tank, and pressure gauges. The driving force is a high-pressure tank of nitrogen with a regulator attached. It delivers a constant pressure of 1080 kPa to a 0.03 m^3 stainless steel tank filled with water. The steady flow is monitored by an orifice flow meter. After setting the desired pressure drop across the orifice with a needle valve, the flow rate is calibrated with a graduated cylinder and stopwatch. The precision of the gauge allows the flow rate to be set to within 0.03 cm^3/s of the desired flow rate. Approximately 30 minutes are required to acquire data at a sufficient number of points within the spray for one test condition. A constant flow over this time is essential to ensure that the spray does not change while it is being characterized.

A phase Doppler particle analyzer (PDPA) was used to measure the local drop size, mean velocity, and volume flux. A description of this system is given by Bachalo and Houser (1984). To decrease the amount of variation in the data, the PMT voltage of the PDPA was kept at a constant setting of 310 volts (McDonell and Samuelsen 1990). A velocity off-shift setting of 3.93 was required in order to measure a velocity range of 0–20 m/s. To obtain an accurate estimation of the spray characteristics nominal sampling rates of 5500 validations/point were used.

The injector is mounted onto a traversing stand that can run in the x, y, and z directions, shown in Figure 1. The spray is moved from one position to another, while the PDPA is kept stationary. Because the spray characteristics change with position, it is important to have the same reference point for each test. The origin of the coordinate axis for the experiment is taken

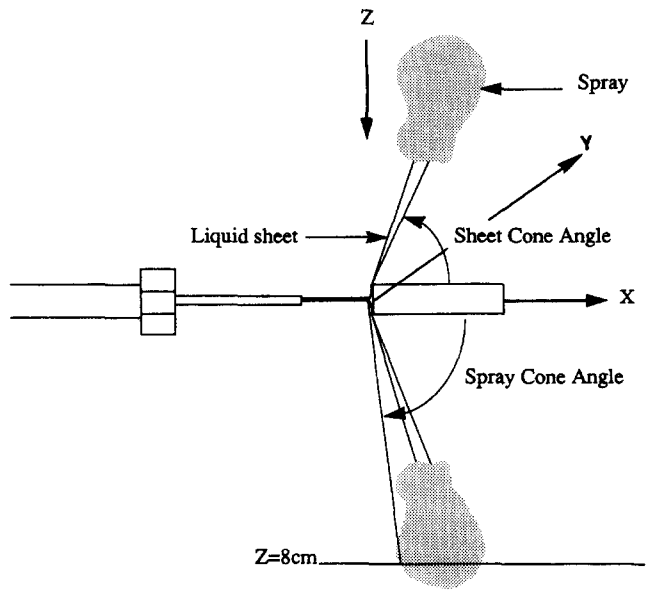

Figure 1 Impinging jet setup and the reference axes

to be the center of the rod. The z-axis is in the vertical direction, and the x-axis is in the direction of the jet. All z and x locations are reported relative to this point (see Figure 1). A digital traverse controller operates the traverse and positions the injector to within 0.025 mm of a desired location. The measurements are taken at 5 mm intervals in the x direction and the spray is traversed from the front edge (smaller x) of the conical spray to the back edge (larger x). Data are acquired only in the region of the spray where the PDPA detects more than 20 drops per second. The mean diameter, velocity, and the local volume flux are recorded simultaneously at 8 cm below the impaction point. At this distance, the sheet is able to break-up and form spherical drops, and the number of ligaments and nonspherical drops in the measurement area is minimized. This is determined by the number of signals that the PDPA rejected. When the probe volume of the PDPA is moved farther below the impingement point, the number of rejections is decreased. The distance at which the number of rejections does not decrease significantly as z changes is $z = 8$ cm. Therefore, this plane is chosen to collect the data. It is assumed that the spray is axisymmetric so no data are taken in the y direction.

Spray cone angle

The front view of the impinging jet atomizer is shown in Figure 2a for a surface to diameter ratio of $\Delta = 2.3$ and $u_j = 8.1$ m/s. A conventional 35-mm camera with side lighting is used to produce these photographs. The figure shows that a radial sheet is formed after the impingement, which becomes unstable and breaks into drops. A wavy structure is formed on the liquid sheet, which emanates from the impingement point and propagates radially outward as concentric circles. Similar wavy patterns were observed by Tanasawa et al. (1958). A magnified image of the edge of the sheet is given in Figure 2b. No regular pattern can be identified at the breakup point, and the sheet disintegrates randomly. A study of the magnified images of the sheet breakup point reveals that the atomization is not governed purely by the growth of the surface waves and the formation of the ligaments (Hagerty and Shea 1955; Huang 1970). It appears that the drops are formed due to the azimuthal instabilities in the liquid rim. The rim of the liquid sheet is rounded due to the surface tension

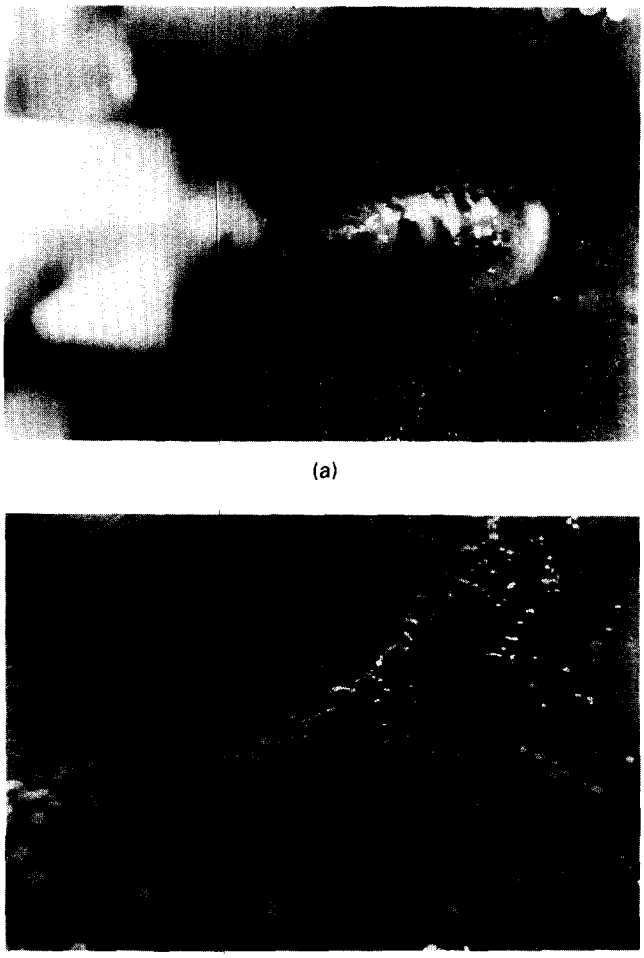

Figure 2 (a) Front view of the impinging jet for $\Delta = 2.3$ and jet velocity = 8.1 m/s; (b) a closeup photograph of the atomization of the liquid sheet

forces, and it is somewhat thicker than the other regions in the sheet. The aerodynamic effects result in the churning of this rim region, and the capillary effects cause its breakup from the sheet. The ligaments later break into small drops by the capillary action (Ashgriz and Mashayek 1995; and Vassallo and Ashgriz 1991). This complex process can not be properly explained by the present models for the liquid sheet breakup due to the Kelvin–Helmholtz type instabilities.

A set of side-view photographs of impinging jets is shown in Figure 3 for jet velocities of 4.3, 5.1, 6.6, and 9.7 m/s, and $\Delta = 2.3$. It is observed that the sheet cone angle increases as the jet velocity is increased. The sheet cone angle is defined as the angle between the sheet and the jet axis (x-axis, see Figure 1). The cone angle depends on the initial jet velocity and the surface-to-jet diameter ratio. The higher the jet velocity, the smaller the thickness of the liquid film formed on the solid surface (Watson 1964). This causes more of the fluid to flow parallel to the face of the rod, and consequently, the cone angle increases. Another observation from Figure 3 is that the liquid sheet is curved more at lower jet velocities. This is due to the action of surface tension forces on the liquid sheet. Because the sheet initially has some curvature towards the jet axis, the surface tension forces are higher on the outer than on the inner surface of the sheet. These unbalanced surface tension forces tend to bend the sheet towards the jet axis. This effect becomes more pronounced as the inertia of the sheet reduces.

Figure 4 shows the variation of the cone angle with the jet Reynolds number. Two different ways are used to measure the cone angle. Figure 4a shows the "sheet" cone angle measured directly from the photographs for two rod sizes with $\Delta = 2.3$ and $\Delta = 5.3$. For both cases, the cone angle increases with the jet Reynolds number; it reaches 79° at a Reynolds number of 10^4. For Reynolds numbers below 10^4, the sheet cone angle is always larger for the smaller rod ($\Delta = 2.3$). However, as Re is increased beyond this point, the trend changes, as shown in Figure 4b. Figure 4b shows the variation of the "spray" cone angle, which is defined as the angle between the x-axis and a line drawn from the impaction point to the point in the spray with the largest volume flux (i.e., 1×10^2 cc/s/cm^2) at $z = 8$ cm, as labeled in Figure 1. The "spray" cone angle increases with increasing jet velocity for all the rods that are tested.

The surface-to-jet diameter ratio Δ affects the cone angle in an interesting way. At high jet velocities (high Re), the cone angle increases with increasing Δ, but at low jet velocities, the opposite occurs. For low jet velocities and small diameter surfaces, the boundary layer in the film on the surface is not well developed, and, therefore, as the liquid separates from the surface it has a larger mean velocity and more momentum in the radial direction as compared to a higher Δ case. Thus, the fluid can overcome the surface tension forces, and the cone angle spreads out. As Δ increases, the boundary layer is further developed, and, therefore, the mean velocity in the radial direction is reduced. For high velocities, the boundary-layer thickness formed on the surface is smaller, and it influences a smaller fraction of the velocity profile. Therefore, the velocity profile is more uniform in this case, and the cone angle is mainly governed by the flow trajectory in the free surface of the liquid. The flow trajectory is turned more for larger Δ, therefore, the cone angle at high jet velocities is larger for the higher Δ.

To derive an empirical relation for the spray cone angle θ, the following arguments are used. The impaction of the jet on the surface results in a stagnation-type flow. We assume that the sheet cone angle $\tilde{\theta}$ is approximately equal to the slope of the free stream at the edges of the splash plate. Therefore, this angle can be approximated by the ratio of the two velocity components: $\tan\tilde{\theta} \approx u_z/u_x$, where u_z and u_x represent the characteristic radial and axial velocities, respectively (see Figure 1). Based on the continuity equation, $u_x/u_z \sim (h/d_j)\Delta$, where h is the thickness of the liquid sheet at the edges of the splash plate. Therefore, the sheet cone angle purely based on the stagnation flow of an inviscid fluid is $\tan\theta = \alpha\Delta$, where α should be determined empirically. The influence of the viscous effects in changing the flow direction is considered by including two terms. One accounting for the overall viscous effects for a constant pressure gradient flow along the radial axis, and another representing the effects of the development of the boundary layer at the solid interface. The first term depends on Re^{-1} and the second term on $\mathrm{Re}^{-1/2}$. Thus, the sheet cone angle (in radians) can be estimated by the following relation:

$$\tilde{\theta} \simeq \tan^{-1}\left[\alpha\left(1 - \frac{\mathrm{Re}_c}{\mathrm{Re}}\right)\Delta + \frac{\beta}{\mathrm{Re}^{1/2}}\right] \tag{3}$$

The spray cone angle, however, is different than the sheet cone angle. The experimental results show that the correction is proportional to Δ; i.e., $\theta' \simeq \tan\theta' \simeq \varepsilon\Delta$. Therefore, the following empirical relation is written for the spray cone angle:

$$\theta \simeq \tan^{-1}\left[\alpha\left(1 - \frac{\mathrm{Re}_c}{\mathrm{Re}}\right)\Delta + \frac{\beta}{\mathrm{Re}^{1/2}}\right] + \varepsilon\Delta \tag{4}$$

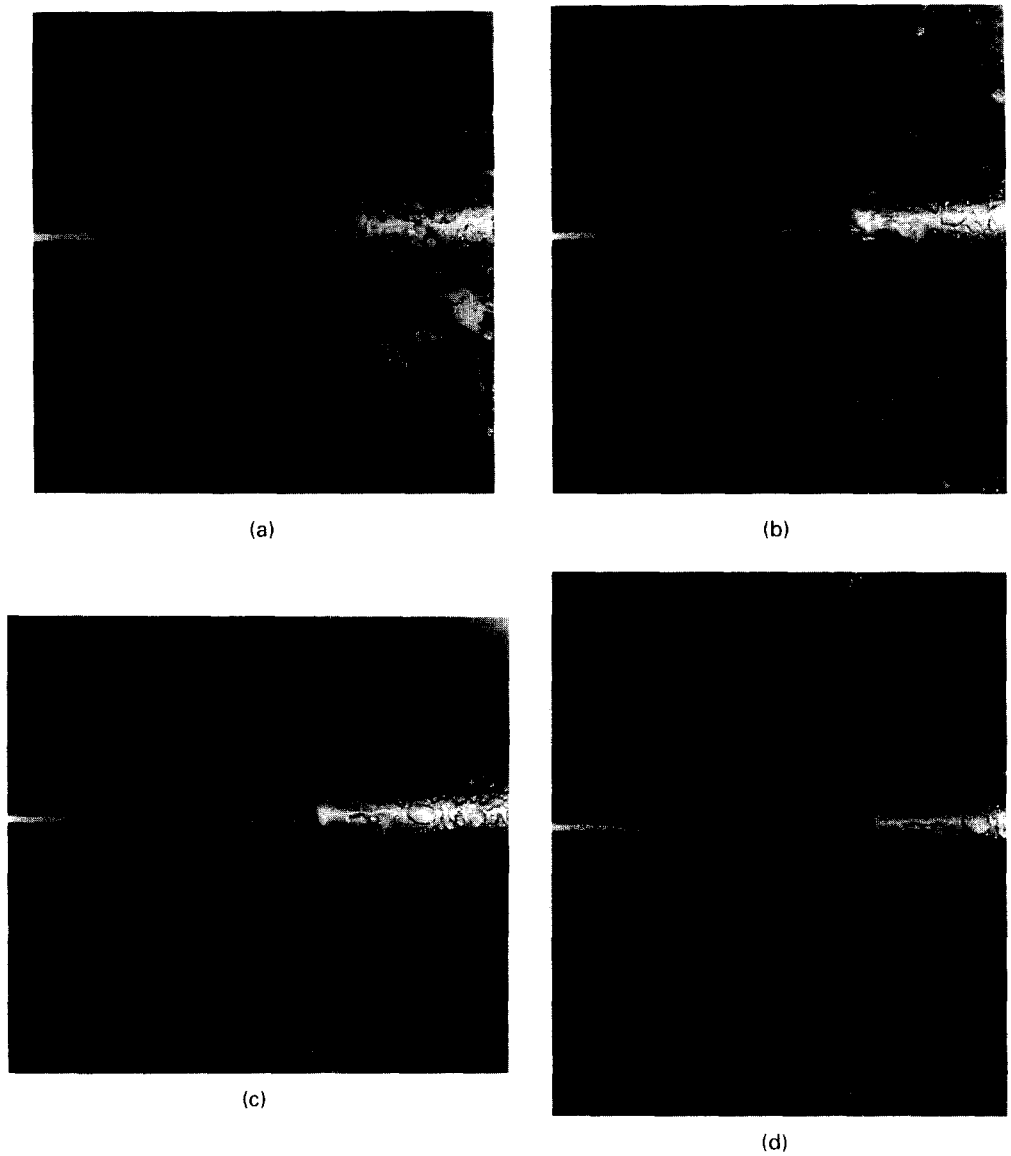

Figure 3 Side views of the liquid sheet cone for $\Delta = 2.3$ and jet velocities of (a) 4.2 m/s; (b) 5.1 m/s; (c) 6.6 m/s; (d) 9.7 m/s

In Equations 3 and 4 $Re_c = 10^4$ is the critical Reynolds number at which point the influence of the Δ on θ changes, $\alpha = 1.7$, $\beta = 500$, and $\varepsilon = 1.2 \times 10^{-2}$. The curves in Figure 4 are obtained from the above correlations. The maximum error of these correlations is within 5°, which is well within the experimental error.

Drop size and velocity segregation

To investigate the effect of the jet velocity and surface-to-jet diameter ratio on the spray character, drop sizes, and velocities are measured using the PDPA system. This type of splash-plate atomization results in the segregation of drop sizes and velocities across the spray. Figure 5 clearly shows the drop size segregation for $\Delta = 3.0$, 8.7, and 13.9, and for different jet velocities. Note that the mean diameter decreases along the x-axis for all cases. This is in contrast to an original expectation of a Gaussian distribution. The reason for the drop size segregation is not clear. It may be due to the mechanism of the sheet breakup where the smaller drops are ejected at a different trajectory than the larger drops. (Some insight about this mechanism is given by Ashgriz and Poo, 1990.) However, the development of air currents within the hollow spray cone may be a better explanation of the observed segregation of the smaller drops. The air currents are generated because of the aerodynamic interaction between the spray and the surrounding atmosphere. The trajectories of the smaller drops are affected more, because the smaller drops have a higher surface-to-volume ratio, and, therefore, they have a higher aerodynamic drag-to-momentum ratio (Poo and Ashgriz 1991; Eroglu and Chigier, 1991).

The changes in the diameter distribution across the spray in the x direction are shown in Figure 6 for the test condition of $u = 14.1$ m/s and $\Delta = 3.0$. The spray formed at this condition has diameters that vary significantly in the x direction. As can be seen from the plots, the range of diameters decreases as x increases. At $x = 20$, 90% of the drops are smaller than 321 μm, while at $x = 50$ mm, 90% are smaller than 103 μm. For the axial positions $x = 25$ mm through $x = 50$ mm the largest number of drops are in the diameter range of 26.6 μm to 37.5 μm. For $x = 20$ mm, however, the largest number of drops are in the range of 168.37 μm to 179 μm.

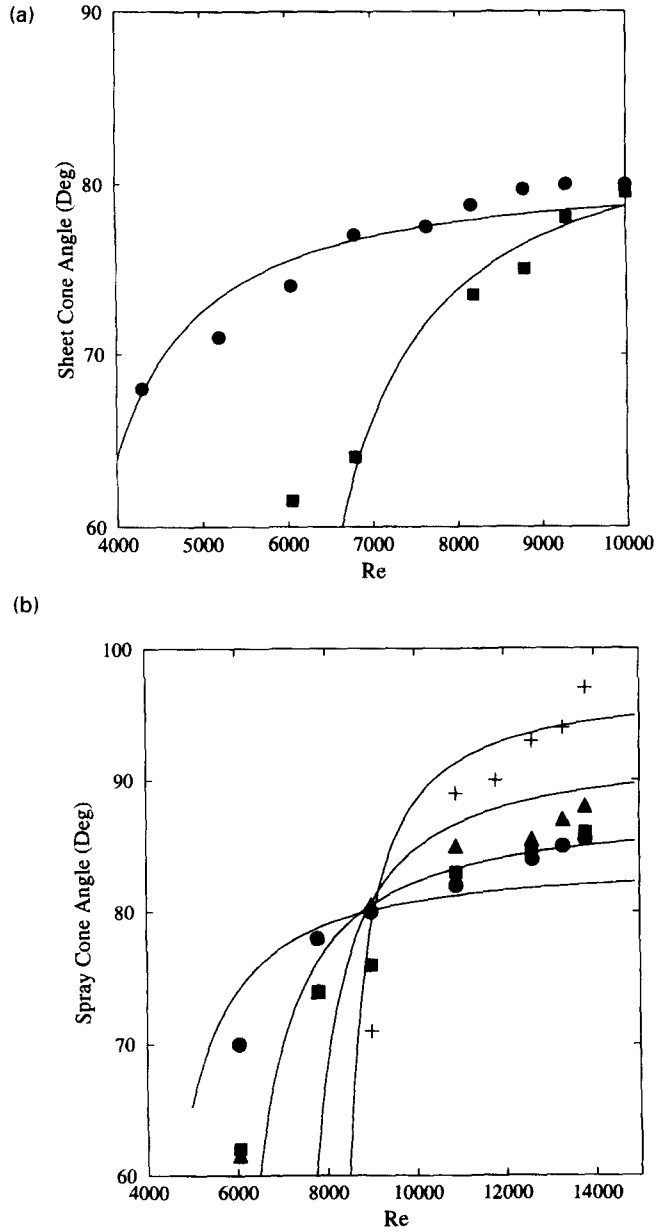

Figure 4 Effect of Reynolds number on the (a) liquid sheet cone angle measured from photographs for $\Delta=2.3$ ●; and $\Delta 5.1$; and (b) spray front cone angle for $\Delta=3.0$ ●, $\Delta=5.1$ ■, $\Delta=8.7$ ▲, $\Delta=13.9$ +

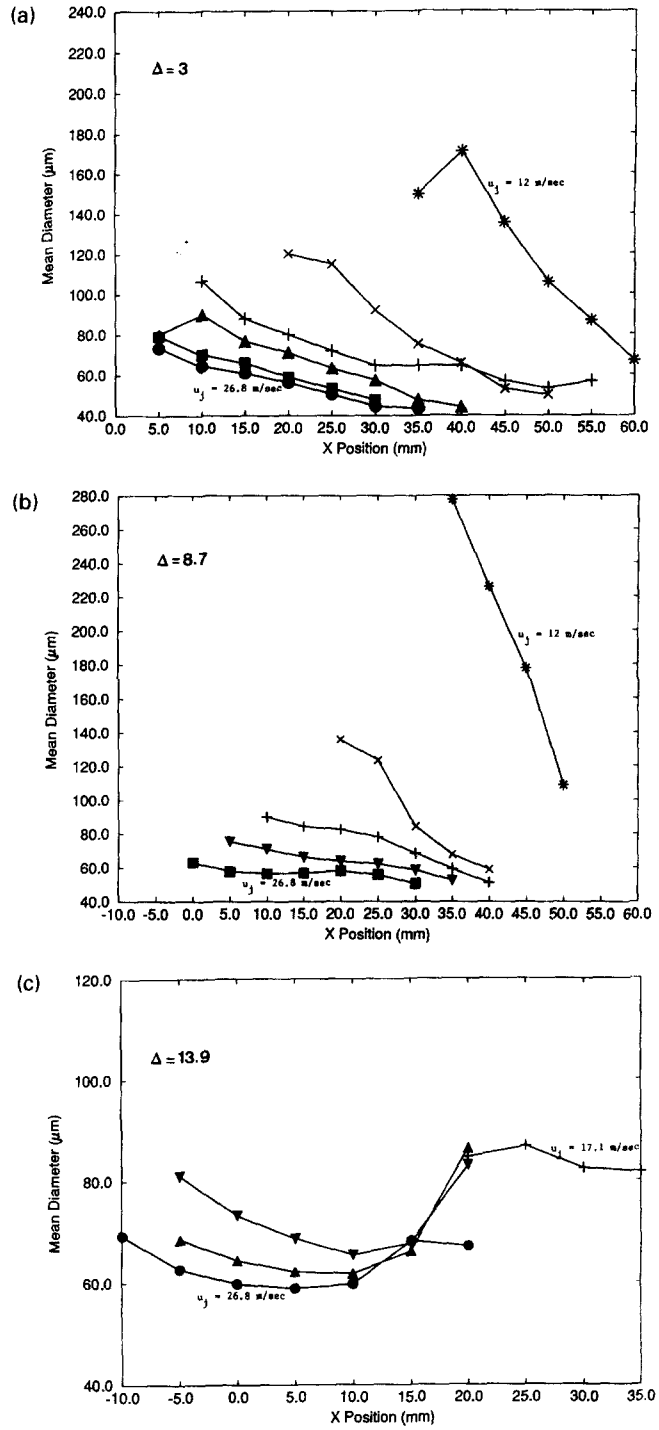

Figure 5 Variation of mean diameter in the axial direction for (a) $\Delta=3.0$: $u_j=12.0$ m/s $*$, $u_j=14.9$ m/s, $\times$, $u_j=17.1$ m/s +, $u_j=21.0$ m/s ▼, $u_j=22.8$ m/s ▲, $u_j=26.8$ m/s ●; (b) $\Delta=8.7$: $u_j=12.0$ m/s $*$, $u_j=14.9$ m/s $\times$, $u_j=17.1$ m/s +, $u_j=21.0$ m/s ▼, $u_j=26.0$ m/s ■; (c) $\Delta=13.9$: $u_j=17.1$ m/s +, $u_j=21.0$ m/s ▼, $u_j=22.8$ m/s ▲, $u_j=26.8$ m/s ●

Figure 5 also shows that as the jet velocity increases the mean diameter generally decreases. As indicated by Inamure et al. (1991), the thickness of the liquid sheet decreases with increasing the jet Reynolds number. In another related experiment, Lefebvre (1989) has shown that the drop size decreases with the liquid sheet thickness. This explains the observed trends in Figure 5. Figure 5 also reveals that the drop sizes become more uniform at higher jet velocities. For a jet velocity of 14.9 m/s and $\Delta = 8.7$ the diameter changes from 136 to 59 μm. As the jet velocity increases, the curves become flatter, and the mean diameter varies by only 15 μm for jet velocities above 22.4 m/s (see Figure 5b). The reduction in the drop segregation is caused by the opening of the cone angle at higher jet velocities, which causes the currents inside the cone to be weaker and the drops to no longer be entrained. In addition, because the atomization process is more efficient at higher jet velocities, the maximum drop size decreases and the range of the drop diameters becomes narrower.

Another observation from Figure 5 is that a larger Δ at high jet velocities generates a more uniform spray. For example, the local mean diameter of the spray for $u_j = 21$ m/s and $\Delta = 3.0$

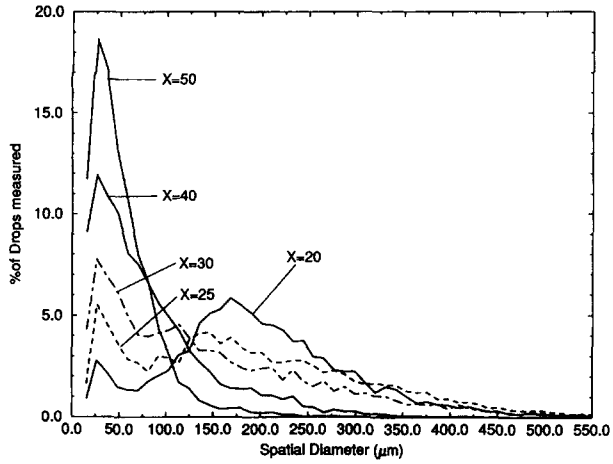

Figure 6 Changes in the drop size distribution for different X locations in the spray

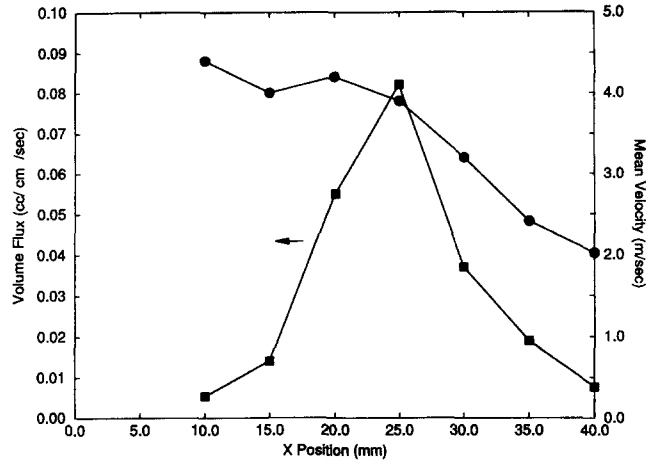

Figure 8 Variation of volume flux and mean velocity in the axial direction; mean velocity in m/s ●, volume flux in cc/cm^2/s ■

changes from 104 to 50 μm along the x-axis. Whereas, the local mean diameter for the same jet velocity but a larger $\Delta = 8.7$ varies from 75 to 52 μm, which is a 23 μm reduction along the x-axis. The change in the mean diameter along the x-axis becomes even smaller for $\Delta = 13.9$ (a 17 μm reduction, from 83 to 66 μm). For smaller jet velocities, the trend is reversed. For $u_j = 12$ m/s the variation of the mean diameter along the x-axis for $\Delta = 3.0$ is from 171 to 67 μm, which is a 104 μm change. At $\Delta = 8.7$ and for the same jet velocity of $u_j = 12$ m/s, the mean diameter decreases by a total of 171 μm, from 277 to 108 μm, as x increases.

The efficiency of the drop size segregation with the jet velocity and Δ has the same trend as the cone angle. It appears that the drop size segregation and the cone angle may be related. As the spray cone angle increases, the size of the hollow zone within the spray cone increases, resulting in the reduction of the velocity of the air currents. The lower the air velocity, the less the drop size separation, and, therefore, the more uniform the spray in the x direction.

Figure 7 shows the mean vertical velocity of the drops along the x-axis at 8 cm below the impingement point ($z = 8$ cm). The jet velocity is varied while the surface to jet diameter is kept constant at $\Delta = 3.0$. The velocity decreases from the front to the back of the spray as the spray is traversed in the positive x direction. Three factors are responsible for the observed velocity decrease in the x direction. One is due to the atomization process, which results in a distribution of drop sizes and velocities. Smaller drops tend to move slower, because they have a higher surface-to-volume ratio and consequently higher drag (Poo and Ashgriz 1991).

The second factor that may be partly responsible for the observed velocity decrease in the x direction is the velocity profile in the sheet after impingement. When the jet impinges on the surface, the boundary layer on the surface continuously grows and results in a nonuniform velocity profile in the sheet when it leaves the surface (Watson 1964). Because the velocity is higher at the sheet surface and reduces towards the inside of the film, the mean velocity of the drops may follow the same trend.

The third factor that results in lower observed velocities along the x-axis is due to the variation of the drop trajectories. The drops are not moving in the vertical direction; however, the PDPA measures only the vertical component of the velocity. The velocity components reduce slightly as the drop trajectory becomes more off axis (i.e., for larger x). However, sample calculations have shown that this cannot be the only factor responsible for the observed reductions in the velocity along the x-axis.

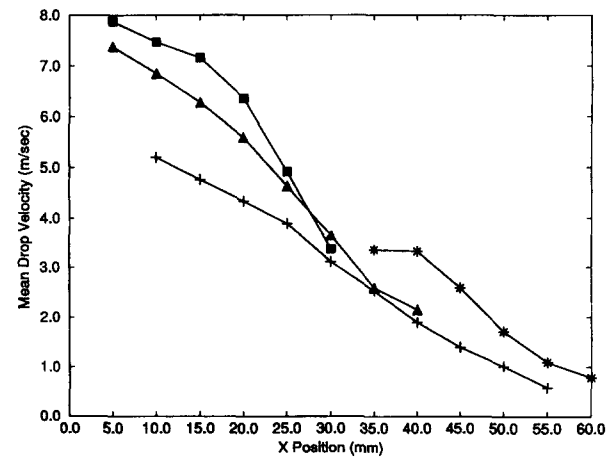

Figure 7 Variation of mean drop velocity in the axial direction for $\Delta = 3.0$: $u_j = 12.0$ m/s *, $u_j = 17.1$ m/s +, $u_j = 21.0$ m/s ▼, $u_j = 26.0$ m/s ■

Mean drop size and velocity

To investigate the effect of the jet velocity on the spray characteristics, the drop mean velocity and diameter at the "center" of several sprays are compared. The "center" of the spray is defined as the location where the volume flux is at its maximum value. This is determined by measuring the volume flux along the x-axis at regular intervals, as shown in Figure 8. By fitting a curve to the volume flux data, the x position at which the maximum occurs can be estimated.

One of the ways that the size of the impaction surface affects the flow is that a larger surface applies more shear stress to the fluid and reduces the mean velocity of the flow. This effect can be seen in Figure 9, which shows the mean velocity of the drops at the center of the spray. The curves show that for $\Delta = 3.0$, a spray with the highest drop velocities is formed; whereas, for $\Delta = 13.9$, a spray with the lowest drop velocities is formed. The point at which a spray had zero velocity was determined by reducing the jet velocity until no sheet was formed from the edge of the rod. At this velocity the fluid travels around the 90° edge

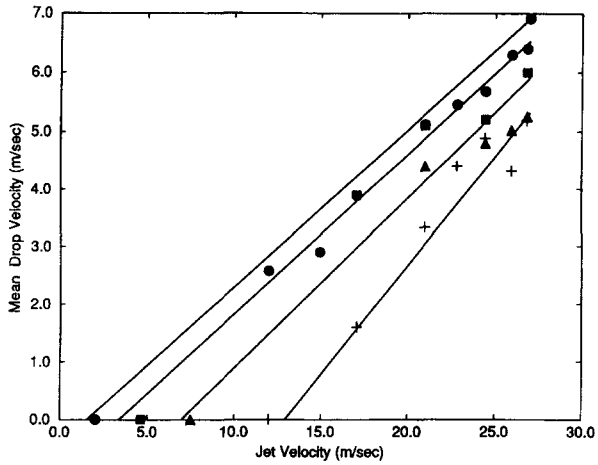

Figure 9 Effect of jet velocity and plate size on the mean velocity at the center of the spray and an empirical fit; $\Delta=3.0$ ●, $\Delta=5.1$ ■, $\Delta=8.7$ ▲, $\Delta=13.9$ +

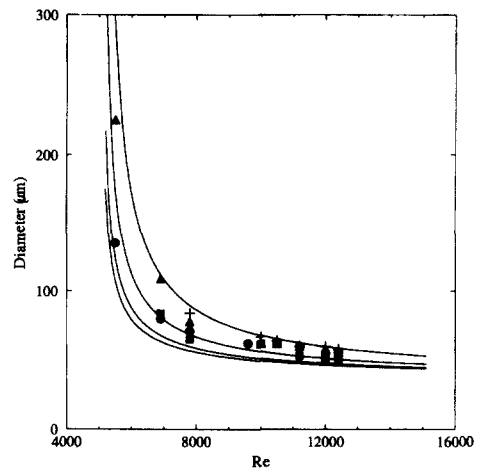

Figure 10 Effect of jet velocity and plate size on the mean diameter at the center of the spray and an empirical fit; $\Delta=3.0$ ●, $\Delta=5.1$ ■, $\Delta=8.7$ ▲, $\Delta=13.9$ +

of the rod and drips off. Drop mean velocities u_d can be correlated by the following relation:

$$u_d = au_j + b \tag{7}$$

where u_d and u_j are in m/s and the experimentally determined coefficients are:

$$a = 0.27 + 10^{-4}\Delta^{2.6} \tag{8}$$

$$b = -0.0729\Delta^{1.55} \tag{9}$$

The lines in Figure 9 are obtained by using Equation 7. Our experimental data indicate that for small Δ, the mean drop velocity is much smaller than the jet velocity. For small Δ, all the terms containing Δ can be neglected, and the drop velocity becomes approximately equal to 1/3 of the jet velocity.

The drop velocity at the breakup point is usually assumed to be equal to the sheet velocity, and the sheet velocity is assumed to be equal to the jet velocity. Taylor (1966) indicates that when the liquid impacts on a surface, the pressure builds up there and deflects the streamlines from the direction of the jet to the lines in the impact plane, which spread out radially from the impact region. The stream velocity varies in passing through this region but, if the fluid is inviscid, regains its original value as it passes out of it. Experimental measurements of the sheet velocity have verified this theory. However, whether the drops at the break-up point have the same velocity as the sheet has not been verified. Our results indicate that the drop velocities at $z = 8$ cm are much smaller than the jet velocity, and consequently, smaller than the sheet velocity. Therefore, part of the observed velocity change is due to the aerodynamic drag. However, sample calculations indicate that not all of this change can be attributed to the drag effect. (Because close to the break-up region there is a significant drop–drop interaction, a proper drag coefficient cannot be determined. Therefore, our sample calculations could only show an approximate value and are not presented here.)

Figure 10 shows how the mean diameter at the center of the spray is affected by the surface-to-jet diameter ratio and the jet velocity. The dashed curve in the figure is obtained from Equation 1 given in Fraser et al. (1962) for sheet breakup. If the densities and the surface tension are assumed to be constant, then Equation 1 reduces to $k/u_j^{2/3}$. The constant k is dependent on the injector. In our case a value of $k = 500$ makes an excellent fit through the datapoints for values of u_j greater than 18 m/s. At these velocities, the size of the impaction surface has little effect on the size of the drops. For lower jet velocities, the mean diameter of the drops at the center of the spray increases when a larger impaction surface is used. The difference between the equation of Fraser et al. and our results is due to the method used to create the sheet. Equation 1 is obtained for sprays formed from a slot-shaped nozzle which creates different sheet thicknesses. However, in the present experiment, the sheet thickness is dependent on both the jet velocity and Δ. For larger rod diameters (i.e., larger Δ) and low velocities the surface shear effects reduce the mean velocity of the sheet, which results in less efficient atomization. As can be seen from Figure 10, there is a greater difference in the mean velocity for different Δ at lower jet velocity. At higher velocities, the shear stress effects become minor, and the results can be well predicted by Equation 1. To account for the effect of jet velocity and surface-to-jet diameter on the mean (linear) drop diameter in jet-on-surface impinging atomizers, the experimental data are used to derive the following empirical relation:

$$d = d_m\left[1 + \frac{K_1}{(\mathrm{Re} - \mathrm{Re}_m)^{2/3}} + \frac{K_2\Delta^2}{\mathrm{Re} - \mathrm{Re}_m}\right] \tag{10}$$

where $d_m = 35$ μm and $\mathrm{Re}_m = 5000$ are the minimum drop size and minimum Reynolds number, respectively, $K_1 = 114$, and $K_2 = 14$. The above correlation has several features. For very small Δs, the third term on the right-hand side is negligible, and we obtain a correlation similar to that of Fraser et al. Equation 1. When Δ is large, the second term is negligible, and we obtain a correlation similar to that of Ingebo (1984), Equation 2. In addition, the first term is added to provide a minimum drop size for very large Reynolds numbers. Equations 1 and 2 provide a drop size of zero as the Reynolds number approaches infinity, which is not physical. The minimum Reynolds number Re_m in Equation 10 represents the Reynolds number below which the liquid sheet does not atomize.

Conclusion

The experimental investigation of jet impinging splash-plate atomizers has revealed that the hollow cone spray formed by these atomizers has the following characteristics. At low jet velocities, larger surface-to-jet diameter ratios Δ cause the cone angle θ to

decrease; however, at large jet velocities, the reverse occurs: an increase in Δ increases θ. The mean diameter and velocity are larger at the outer periphery of the spray cone and decrease towards the spray axis. It is suggested that this size and velocity segregation is caused by the air currents generated by the spray inside the spray cone. The efficiency of the drop segregation is found to be directly dependent on the spray cone angle. The spray becomes more uniform at higher jet velocities and larger surface-to-jet diameters. Based on these results, it can be concluded that the drop sizes and velocities can be segregated in a controlled manner by changing the jet-to-surface diameter ratio and manipulating the design of the afterbody of the impinging surface. The interaction between the spray flow and the body of the impinging surface can cause different air (gas) currents, which will entrain and segregate drops. Such atomizers will result in simultaneous atomization and separation of drops or particles.

In addition, the mean diameter at the region of the spray with the highest local volume flux, referred to as the "center" of the spray, decreases with increasing jet velocity. For low jet velocities (less than 18 m/s), a larger Δ generates sprays with larger drops; however, for high jet velocities, Δ does not have a significant effect on the mean drop diameter. Finally, the mean velocity of the drops increases with increasing jet velocity and decreases with increasing Δ. Empirical correlations are provided for the variation of the mean drop size and velocity as a function of the Reynolds number and Δ.

References

Ashgriz, N. and Poo, J. Y. 1990. Coalescence and separation in binary collisions of liquid drops. *J. Fluid Mech.*, **221**, 183–204

Ashgriz, N. and Mashyek, F. 1995. Temporal analysis of capillary jet breakup. *J. Fluid Mech.*, **291**, 163–190

Bachalo, W. D. and Houser, M. J. 1984. Phase Doppler spray analyzer for simultaneous measurements of drop size and velocity distributions. *Optical Eng.*, **23**, 583–590

Dixon, B. E., Russell, A. W. and Swallow, J. E. 1952. Liquid films formed by means of rotating disks. *Br. J. Appl. Phys.*, **3**, 115–119

Dombrowski, N. and Hooper, P. C. 1963. A study of the sprays formed by impinging jets in laminar and turbulent flow. *J. Fluid Mech.*, **18**, 392–400

Donaldson, C. D. and Snedecker, R. S. 1971. A study of the sprays formed by impinging jets in laminar and turbulent flows. *J. Fluid Mech.* **45**, 281

Eroglu, H. and Chigier, N. 1991. Initial drop size and velocity distributions for air blast coaxial atomizers. *J. Fluids Eng.*, **113**, 453–459

Fraser, R. P., Shea, P., Dombrowski, N. and Hasson, D. 1962. Drop formation from rapidly moving liquid sheets. *AIChE J.* 672–680

Hagerty, W. W. and Shea, J. F. 1955. A study of the stability of plane fluid sheets. *J. Appl. Mech.*, **22**, 509–514

Heidmann, M. F., Priem, R. J. and Humphrey, J. C. 1957. A study of sprays formed by two impinging jets. NACA Technical Note 3835

Huang, J. C. P. 1970. The break-up of axisymmetric liquid sheets. *J. Fluid Mech.*, **43**, 305–319

Ibrahim, E. A. and Przekwas, A. J. 1991. *Impinging jets atomization. Phys. Fluids A*, **3**, 2981–2987

Inamure, T., Nagai, N., Sunanaga, H. and Masubuchi, M. 1991. Spray flow characteristics in air blast atomization. *Transactions of the Japan Society of Mechanical Engineers*, **B57**, part I, 1327–1331; part II, 1332–1339

Ingebo, D. 1984. Atomization of liquid sheets in high pressure airflow. NASA TM-83731, NASA-Lewis Research Center, Cleveland, OH

Lefebvre, A. H. 1989. *Atomization and Sprays*. Hemisphere, Bristol, PA

McDonell, B. and Samuelsen, S. 1990. Sensitivity assessment of a phase-Doppler interferometer to user-controlled settings. In *Liquid Particle Size Measurement Techniques:* Vol. 2. E. D. Hireman, W. D. Bachalo, and P. G. Felton, eds., 170–218, American Society of Testing Materials (ASTM STP 1083), Philadelphia, PA

Poo, J. Y. and Ashgriz, N. 1991. Variation of drag coefficients in an interacting drop stream. *Exp. Fluids*, **11**, 1–8

Rayleigh, J. W. S. 1945. *The Theory of Sound*, Vol. 2. Macmillan, New York

Ryan, H. M., Anderson, W. E., Pal, S. and Santoro, R. J. 1995. Atomization characteristics of impinging liquid jets. *J. Propulsion Power*, **11**, 135–145

Tanasawa, Y., Sasaki, S., and Nagal, N. 1958. The atomization of liquids by flat impingement nozzles. *Eng. Digest*, **19**, 151–155

Taylor, G. I. 1960. Formation of thin flat sheets of water. *Proc. R Soc. Lond. A*, **259**, 1–17

Taylor, G. I. 1966. Oblique impact of a jet on a plane surface. *Philos. Trans. Roy. Soc. London Ser. A*, **260**, 96–100

Vassallo, P., Ashgriz, N. and Boorady, F. A. 1992. Effect of flow rate on the spray characteristics of impinging water jets. *J. Propulsion Power*, **8**, 980–986

Vassallo, P. and Ashgriz, N. 1991. Satellite formation and merging in liquid jet breakup. *Proc. R. Soc. Lond. A*, **433**, 269–289

Watson, E. J. 1964. The radial spread of a liquid jet over a horizontal plane. *J. Fluid Mech.*, **20**, 481–499